Monitoring of Two Unvented Roofs with Air-Permeable Insulation in Climate Zone 2A

Kohta Ueno
Associate Member ASHRAE

Joseph W. Lstiburek, PhD, PEng
Fellow ASHRAE

ABSTRACT

Unvented roof assemblies can bring attic mechanical systems into conditioned space, negating ductwork losses. However, in previous work, unvented roofs with air-permeable (fibrous) insulation, instead of air-impermeable insulation (spray foams) have shown localized moisture accumulation at the ridge. This research is a test implementation of two unvented roof assemblies insulated with air-permeable insulation (netted and blown fiberglass or adhered fiberglass) in hot/humid climates. One test roof is located in Houston, TX and has asphalt shingles; the other is in Orlando, FL, with concrete tile; both are in Climate Zone 2A. Given that localized moisture accumulation and failures occurred at the ridge in previous unvented roofs, a diffusion vent (open to water vapor but closed to airflow) was installed at the highest points in the roof assembly to allow for the wintertime release of moisture. The diffusion vent is an opening at the ridge and hips covered with a water-resistant but vapor-open membrane. As a control comparison, portions of the roof were constructed as a typical unvented roof (self-adhered membrane at ridge).

Collected data indicate that the diffusion vent roof shows greater moisture safety and less wintertime moisture accumulation than the conventional, unvented roof design. The unvented roof had winter periods of 95%–100% rh, with other sensors indicating possible condensation; high moisture levels were concentrated at the roof ridge. In contrast, the diffusion vent roofs had drier conditions. In the spring, as outdoor temperatures warmed, all roofs dried well into the safe range (10% MC or less).

INTRODUCTION

Unvented roofs (also known as *cathedralized attics*) are an established concept in residential building; such roofs are typically implemented with spray polyurethane foam (SPF) at the underside of the roof deck (Rudd and Lstiburek 1998; Lstiburek 2006; Lstiburek 2011). Primary advantages to this construction are that (a) the attic ductwork and heating, ventilating, and air-conditioning (HVAC) system are brought into the thermal and air barrier of the conditioned space, and (b) air leakage at the ceiling plane (often complicated by interior detailing) is eliminated, which typically results in improved overall airtightness. Advantages in hurricane-prone areas include reduced wind-driven rain entry, by eliminating attic vents, and potentially reduced hurricane blow-off issues, due to differential pressurization. Disadvantages include higher first cost and greater surface area (conductive losses); the latter factor is often negated by eliminating duct leakage to the exterior.

However, unvented roof assemblies have a higher risk of wintertime interstitial (hidden) condensation issues than vented roof assemblies. These condensation risks occur when the roof sheathing is colder than interior dew point; in contrast, vented roof assemblies remove interior-sourced moisture before it can condense on the roof sheathing. These risks are addressed in current building code with the requirement for a minimum amount of air-impermeable insulation—such as rigid continuous insulation or spray foam—on the exterior side of the roof assembly. This exterior insulation raises the temperature of the condensing surface, or the underside of the air-impermeable insulation. The air-impermeable insulation requirements are presented (by climate zone) in

Kohta Ueno is a senior associate and **Joseph W. Lstiburek** is a principal at Building Science Corporation, Westford, MA.

Section R806.4, "Unvented Attic Assemblies," of the International Residential Code (ICC 2009). For Climate Zones (CZs) 1A and 2A, the requirement is a minimum of R-5 (RSI 0.9). For reference, requirements for ventilated roof assemblies are covered in Sections R806.1 through R806.3 (ICC 2009).

This research covers two test implementations of unvented roofs in hot/humid climates (CZ 2A): one in Houston, TX, with asphalt shingle roofing, and the other in Orlando, FL, with concrete tile roofing. The roofs were insulated with air-permeable fiberglass insulation, with a diffusion vent detail at the ridge to allow for wintertime removal of accumulated moisture. One goal of the research was to determine the assembly's resistance to condensation, or the design's moisture safety. This research has an additional benefit of potentially reducing the first cost of unvented roofs by eliminating SPF, which is a higher-cost material than fibrous insulations. This research is covered in detail in Ueno and Lstiburek (2015a; 2015b).

PREVIOUS FIELD WORK

The authors made discoveries on the hygrothermal behavior of unvented roofs in hot/humid climates during field implementation; several of these roofs were built in Houston, TX circa 2001 (CZ 2A). The typical roof assembly was asphalt shingle, roofing felt, oriented strand board (OSB) sheathing, and netted and blown cellulose insulation. During the first fall season of operation, a homeowner reported seeing moisture condensation and dripping from the ridge of the unvented attic, from the interior. Field investigation (Figure 1, left) revealed elevated wood moisture contents (MCs) at the ridge and evidence of previous condensation (i.e., rusted staples). The cellulose insulation at the peak had a noticeably "packy" or compactable texture as opposed to the fluffy texture of dry cellulose, indicating previous wetting (Rose and McCaa 1998). This failure was localized at the peak/ridge of the roof. These moisture issues were remediated by removing the insulation at the roof ridge, which solved the problem, but with an associated thermal penalty.

A similar issue arose in two production homes in Jacksonville, Florida (CZ 2A) circa 2000. Again, the roof assembly was asphalt shingles, roofing felt, OSB sheathing, and netted and blown cellulose insulation. During a site visit, the cellulose and roof sheathing were wet to the touch, and the steel truss plate was corroded; however, the wood had not decayed (Figure 1, right). In response, the insulation was removed near the ridge (roughly 2 ft [610 mm]) to increase surface temperatures of the roof sheathing. This roof has been rechecked in 2003 and 2014; roof sheathing conditions remain dry.

Similar localized ridge problems (colloquially referred to as *ridge rot*) have been documented in unvented compact cellulose roof assemblies in northern California (CZ 3C). Lower portions of the roof were dry and undamaged.

BACKGROUND LITERATURE

An overview of the use of dense-pack cellulose insulation (Lstiburek 2010) shows examples of the problems that can occur when using the material in compact roof assemblies. A comprehensive analysis of the use of dense-pack insulation of compact roofs (Schumacher and LePage 2012) noted the potential for interior air-leakage-sourced condensation in cold and mixed climates. Their hygrothermal analysis suggests that failures are not endemic in houses retrofitted with dense-packed roofs, because only moderate airtightness is achieved. Therefore, interior moisture generation is sufficiently diluted by wintertime air leakage to result in low wintertime interior relative humidity (RH) levels.

(a) **(b)**

Figure 1 *(a) Unvented cellulose roof ridge moisture content measurements in Houston, TX and (b) corrosion of ridge truss plate in Jacksonville, FL.*

Salonvaara et al. (2013) ran hygrothermal simulations models of vented and unvented roof assemblies in various configurations in CZs 1 through 4. Interior RH levels were set at design conditions; the roof assemblies consisted of asphalt shingles, felt paper, OSB sheathing, and insulation (open cell SPF [ocSPF] or fiberglass). Cases were run for no water intrusion and for a rainwater leak at the roof sheathing. The authors concluded that a vented attic assembly has better drying ability than unvented assemblies in all climates. Most unvented ocSPF assemblies had safe moisture contents (MCs) without rainwater leakage, but in colder climates (CZ 4) with very vapor-open ocSPF (54 perm in. or 78 ng/[Pa·s·m]), peak MCs reached risky levels. With the addition of rainwater leakage, MCs were substantially higher, resulting in failure in most CZs. The addition of a 1 perm (57 ng/[Pa·s·m^2]) vapor retarder coating on the interior side of the ocSPF resulted in lower MCs without rain leakage, due to reduction of interior-sourced vapor flow). However, the addition of a vapor retarder resulted in higher MCs with rainwater leakage, due to reduced inward drying. Two final cases used blown fiberglass insulation (100 perm in. [145 ng/(Pa·s·m]) instead of ocSPF: when vapor-open interior netting was used for installation, acceptable MCs were found in CZs 1 and 2, but riskier conditions were seen in CZs 3 and 4. Adding netting with a vapor permeance of 10 perms (570 ng/[Pa·s·m^2])] reduced risks to reasonable levels in CZs 1 through 3.

Boudreaux et al. (2013) presented data collected at eight houses in CZs 3A and 4A (four with vented attics and four with sealed attics) to understand their moisture performance. Their data showed that attic absolute moisture levels (vapor pressures) were consistently higher in the sealed attics than in the vented attics. Similarly, the vapor pressures in the main spaces were higher in the sealed attic houses. When the individual house data were plotted, the two groups overlapped. The worst-performing unvented attic had the highest air leakage (10 ach$_{50}$) of the sample; the authors described other factors that influenced interior moisture levels, including occupant density and cooling setpoint. Plots of vapor pressure at various sections of the roof assembly indicated that the sealed attic roof typically had patterns of daytime drying (desorption into the attic, driven by solar gain) and nighttime wetting (adsorption from the attic air). Several sources of moisture for the sealed attic were discussed, including roof sheathing storage, solar-driven moisture from moisture stored in asphalt shingles (judged unlikely by the authors), and exterior air leakage (likely, given the downward stack effect during the summer).

Lstiburek (2014) discussed unvented attics, or an alternate term of *conditioned attic*. In earlier construction, attic ductwork was typically leaky and supply leakage would slightly pressurize the attic. This would cause air leakage (i.e., air communication) from the attic to the main space, thus diluting attic moisture with drier air.

The moisture source in the attic was primarily from interior, rather than exterior sources. Moisture would concentrate in the attic because the moisture-laden air was more buoyant (less dense) than dry air. But as airtight ductwork became more common, incidental space conditioning provided to unvented attics due to communication between the attic and the main space decreased. The resulting problem has been higher humidity levels in unvented and sealed attics, especially with vapor-open insulation materials. Interior moisture is adsorbed and desorbed from the roof sheathing with daily warm and cold cycles. When air communication is eliminated or reduced, moisture accumulates in the attic due to moisture buoyancy. The author also mentions Houston-area field research about the effect of vapor-permeable and vapor-impermeable shingle underlayments on inward vapor drives; the study found no measurable differences between these roof test bays. The author concludes that shingle inward vapor drive issues are not a significant moisture source.

Pallin et al. (2014) built on Boudreaux et al.'s (2013) field studies, running whole-house energy, moisture, and airflow simulations of unvented roof houses, followed by one-dimensional hygrothermal models of air leakage into the unvented roof assembly. The authors ran over 400 simulations, changing variables such as leakage areas, duct leakage, and interior moisture generation rates. The simulations indicated that low interior moisture generation rates present no significant risks, moderate generation rates result in some risky cases, and high generation rates result in some noticeable failure cases. Lower enclosure leakage was associated with higher risks (which retain interior moisture generation in winter), as was midrange attic-to-exterior air leakage. These simulations showed no effect of duct leakage on moisture risks; these failures occurred in winter, when cooling system dehumidification would not reduce interior moisture loads. Based on these simulations, the authors recommended that unvented attics should be built to be as airtight as possible, and interior moisture generation rates should be controlled. They noted that higher air attic-to-exterior air leakage rates—as occur in practice—have moisture risks.

SITE DESCRIPTIONS, TEST ASSEMBLIES, AND INSTRUMENTATION

Two unvented test roofs were built and instrumented (Figure 2). One was in Friendswood, TX (Houston area, CZ 2A); it is a two-story, 4028 ft^2 (374 m^2), slab-on-grade model house that was unoccupied during testing. The other was a two-story, 3600 ft^2 (334 m^2) slab-on-grade house in Orlando, FL, and was occupied after completion of construction.

Both test houses had unvented/sealed attics that were insulated at the roofline. An experimental diffusion vent detail was installed at the ridge, which allows for vapor diffusion drying at the ridge and tops of hips, while preventing airflow/air leakage; it is discussed in detail below. As a

control comparison, one portion of the roof was constructed as a typical unvented roof, with vapor-impermeable, self-adhered membrane at the ridge (a Class I vapor barrier). The team's hypothesis is that moisture accumulation would occur in the control roof, and the experimental diffusion vent roofs would show sufficient drying to avoid failure. Both roofs were insulated with fiberglass insulation, which is air permeable and vapor permeable (in the range of 120 perm in. [170 ng/(Pa·s·m)]).

The Houston roof (Figure 3, left) was insulated with spray-applied/adhered fiberglass (1.8 lb/ft^3 [29 kg/m^3] density) that was left exposed, with no interior finish. The roof assembly consists of asphalt shingles, underlayment (#15 asphalt saturated felt), 7/16 in. (11 mm) oriented strand board (OSB) sheathing, and spray-applied fiberglass at R-38 (RSI 6.7), encapsulating the 2 × 8 (typical) rafters.

The Orlando roof (Figure 3, right) roof assembly consists of concrete barrel tile screwed down to the sheathing, self-adhered modified asphalt 60 mil roofing underlayment with a woven polyester surface, ½ in. (12 mm) plywood sheathing, and blown fiberglass insulation (R-38/RSI 6.7) supported by netting stapled to the roof truss top chords (Owens Corning 2015).

No intentional space conditioning was provided in the unvented attic spaces; the space "floats" at conditions between the interior setpoint and exterior conditions. In the Houston attic, humidification was provided in the final (third) winter, to substitute for the lack of moisture generation at the unoccupied model house.

(a) **(b)**

Figure 2 *Front views of (a) Houston, north elevation, and (b) Orlando (west elevation) test roof houses.*

(a) **(b)**

Figure 3 *Attic interiors: (a) spray-applied fiberglass in Houston and (b) netted/blown fiberglass in Orlando.*

Ridge-Top Diffusion Port Design

The experimental roof assembly at this site has a diffusion vent detail, which allows for vapor diffusion drying at the ridge and tops of hips, while still functioning as an air barrier. The detail is used at the peak of the roof rafter bay cavities (at the ridge and hip conditions); it was not used at the roof valleys. The construction details for Houston and Orlando are shown in Figure 4 and Figure 5.

In both roofs, a portion of the roof sheathing (±3 in. [76 mm]) near the ridge was omitted, similar to typical a slot vent roof ridge detail. This opening was covered with a strip of a highly vapor-permeable roof membrane, composed of a tear-resistant polyethylene terephthalate fabric with a diffusive waterproof dispersion coating. The manufacturer's specified vapor permeance is 214 perms (12,200 ng/[Pa·s·m^2]) dry cup and 550 perms (31,500 ng/[Pa·s·m^2]) wet cup. The membrane was taped to the roof sheathing to create an air barrier and detailed to shed water. At the roof hips of the Houston house, a series of 2 in. (51 mm) diameter holes were drilled in the roof sheathing at the top 2–3 ft (610–915 mm) of the hip. The structural engineer did not accept the omitted sheathing detail at the hips but accepted the drilled hole detail. The slot vent detail was accepted at the roof hips in Orlando. The diffusion vent was covered with typical ridge vent materials, per local practice.

Test Roof Designations

Test roofs were instrumented to capture multiple roof orientations, roof geometries, and ridge materials (diffusion vent versus nondiffusion vent). Instrumentation was typically concentrated the ridge, because moisture typically accumulates at roof peaks. This is referred to as a *ridge package* composed of sensors, shown in Figure 6.

The measurements at the Houston roof (Table 1) include comparisons between roof ridges with diffusion vents and

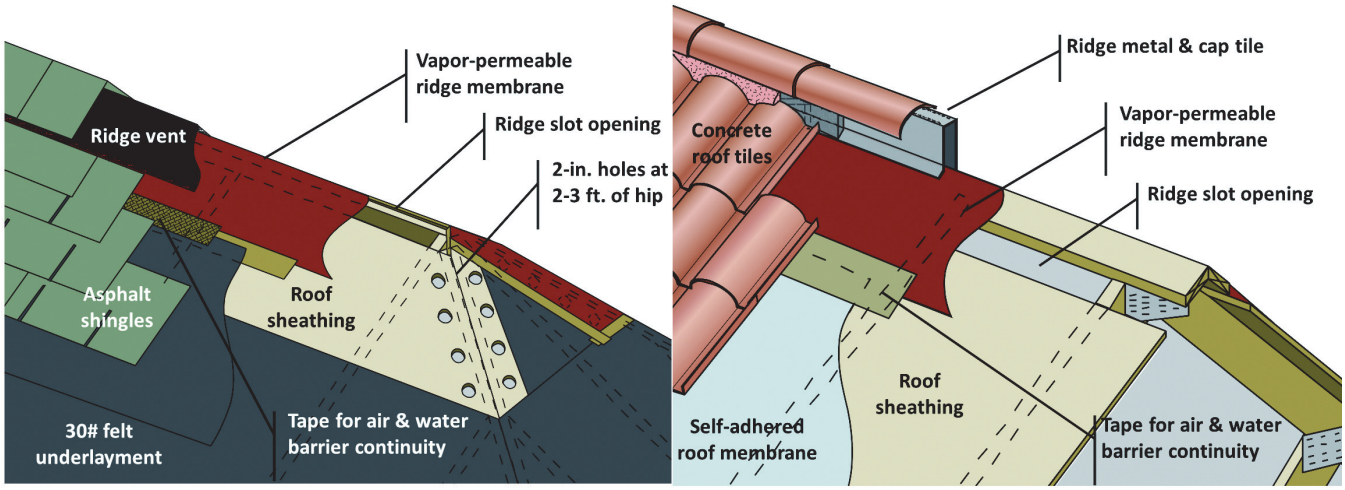

Figure 4 *Ridge (and hip) diffusion vent design: (a) with asphalt shingle in Houston and (b) concrete tile and self-adhered membrane in Orlando.*

Figure 5 *Diffusion vent details (left to right): Houston asphalt shingle diffusion vent ridge detail; Houston hip detail with ridge vent; Orlando tile roof ridge detail, with ridge metal tile support.*

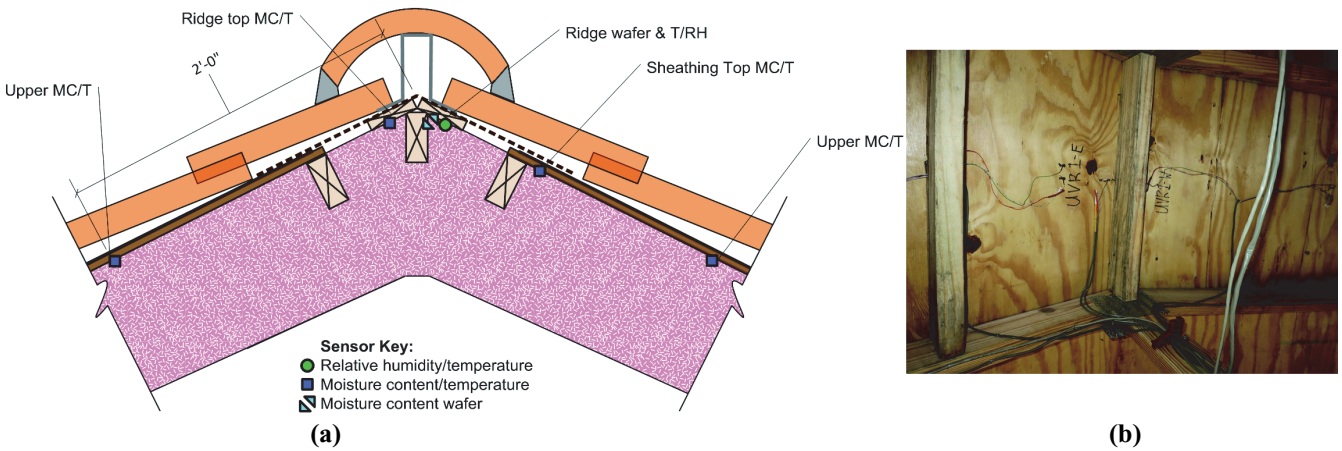

Figure 6 *(a) Diagram of ridge package of instrumentation for Orlando (tile) roof and (b) photo of ridge package.*

unvented (self-adhered membrane) at the ridge. Hip conditions were also measured. The attic geometry includes a larger attic on the east side and smaller attic on the west side. The two attics are connected via a small passage.

The measurements at the Orlando roof (Table 2) had a similar comparison of diffusion vent and unvented ridge conditions and hips. In addition, two roof-wall (RW) conditions (without diffusion vents) were monitored; one with a long run of downhill roof, another with a short run. The house has a smaller attic over the second floor and a larger attic over the first floor that is not covered by the upper story.

Sensor Setup and Data Acquisition System

Measurements in the roof assemblies included temperature and relative humidity (RH), wood sheathing moisture content, and a wood wafer sensor intended as an RH surrogate and condensation indicator. The latter is a wood-based relative humidity surrogate sensor, described in detail by Ueno and Straube (2008); the moisture content of the wood (eastern white pine) is measured via electrical resistance. A typical ridge package is shown below in Figure 6.

Roof sheathing MCs on both sides of the ridge were measured roughly 24 in. (610 mm) from the ridge to capture the extent of the wetting. In addition, at each rafter/truss bay with a ridge package, sheathing MC and temperature are measured lower (or downhill) on the roof sheathing; the number of measurements depended on the roof geometry. These "downhill" MCs measure the moisture accumulation in the rafter bays with the same condition but lower on the roof.

In addition, conditioned attic (i.e., interior) temperature and RH were measured at three pairs of locations; measurements were taken high and low (roughly the 1/3 and 2/3 vertical points) to capture the effects of thermal and/or moisture stratification in the space. Interior main space temperature and RH were measured via a sensor installed in the return duct of the space-conditioning system near the interior grille. Exterior temperature and RH were recorded on site.

Table 1. Houston (Asphalt Roof) Monitoring Locations

Designation	Description	Attic
DVR1	Diffusion vent ridge	East (larger) attic
UVR1	Unvented (control) ridge	East (larger) attic
DVR2	Diffusion vent ridge	West (smaller) attic
UVR2	Unvented (control) ridge	West (smaller) attic
DVR3	Diffusion vent ridge	East (larger) attic
DVH4	Diffusion vent hip	East (larger) attic
DVH5	Diffusion vent hip	East (larger) attic
DVR6	Diffusion vent ridge	West (smaller) attic

Table 2. Orlando (Tile Roof) Monitoring Locations

Designation	Description	Attic
UVR1	Unvented (control) ridge	Upper (over 2nd)
DVR1	Diffusion vent ridge	Upper (over 2nd)
DVR2	Diffusion vent ridge	Upper (over 2nd)
DVR3	Diffusion vent ridge	Lower (over 1st; front of building)
DVH1	Diffusion vent hip (lower)	Lower (over 1st)
DVH2	Diffusion vent hip (upper)	Lower (over 1st)
RW1	Roof wall, no diffusion vent (long roof downhill)	Lower (over 1st)
RW2	Roof wall, no diffusion vent (short roof downhill)	Lower (over 1st)

Data were collected by a measurement and control system installed in the attic. Measurements were taken at five-minute intervals and average values recorded hourly; data were downloaded remotely. No battery backup for the data logger was provided; however, the unit has nonvolatile memory, and resumes data collection after a power failure.

Further information on these monitoring methods is provided in Straube et al. (2002).

Houston Attic Humidification

Given the unoccupied condition of the model house in the Houston roof house, no moisture generation occurred, resulting in lower than expected interior RH levels. Therefore, between the second and third winter, a humidification system was installed in the attic to simulate occupant moisture generation. A heated reservoir-style humidifier was commissioned; by mid-October 2015, it was generating a steady 22.6 lb/day (10.3 L/day). Based on ASHRAE Standard 160 (ASHRAE 2009), this is slightly less than the design moisture generation rate for a two-bedroom residence. Although this is a five-bedroom house, this rate was considered a reasonable moisture generation rate for a source directly introduced to the attic.

AIR LEAKAGE TESTING

As part of the commissioning process, both experimental houses and attics were tested for air leakage. Energy Conservatory instruments (Minneapolis Blower Door Model 3 and DG-700 Pressure and Flow Gauge; ± 3% flow accuracy) were used for multipoint depressurization testing. Full descriptions of the air leakage testing regimen and results are provided in Ueno and Lstiburek (2015a; 2015b).

The Houston house was tested with the attic hatch either open or closed; the air leakage measurements are normalized based on an area/volume takeoff that includes the entire attic. Results are shown normalized by volume (air changes per hour at 50 Pa [ach_{50}]) and surface area (cfm_{50}/ft^2 [$L/s{\cdot}m^2$] enclosure area) and are stated in terms of equivalent leakage area (EqLA) in Table 3. EqLA provides a physical indication of the relative leakage areas of successive tests (Energy Conservatory 2012). Opening the hatch caused the air leakage to increase by only 14%. In both cases, air leakage was less than 0.25 cfm_{50}/ft^2 (1.2 $L/s{\cdot}m^2$) and fewer than 2.5 ach at 50 Pa (half or less than the 5 ach_{50} requirement in the 2012 IECC (ICC 2012) for CZs 1 and 2). The pressures across closed attic hatches were measured with the main space at –50 Pa to demonstrate the relative leakage connection to the interior versus the exterior. The attic-to-exterior pressure drop was 76% to 86% of the total, which is consistent with the hatch open/closed results, or a relatively airtight attic.

Table 3. Houston (Asphalt Shingle) Air Leakage Measurements

	cfm_{50} (L/s)	ach_{50} (h^{-1})	cfm_{50}/ft^2 ($L/s{\cdot}m^2$)	EqLA, in^2 (m^2)
Hatch Closed	2494 (1177)	2.2	0.22 (1.1)	257 (0.166)
Hatch Open	2846 (1343)	2.5	0.25 (1.2)	293 (0.189)

Overall, the roof plane was relatively airtight; using an infrared camera during depressurization, few thermal anomalies were seen at the roof plane. Indoor/outdoor temperature differences were 21°F to 31°F (11.7°C to 17.5°C) during these observations; although the roof was heated by morning sun, induced air leakage was clearly visible. Infrared observation of the roof peaks showed no indications of air leakage at the diffusion vent details. However, leakage often occurred at transitions and connections between roofs and walls, especially at complicated details with multiple intersecting planes. For instance, leakage was evident at dormer and gable end intersecting planes at the front of the house and roof-wall connections at the rear of the house (Figure 7).

The Orlando roof geometry included an upper attic, over the second floor, and a lower attic, at the first floor where it was not covered by the second floor. The house was tested with the two attic hatches open and closed in various combinations, as shown in Table 4. The overall house airtightness with both attic hatches open was 7.6 ach_{50} or 0.58 cfm_{50}/ft^2 (2.9 $L/s{\cdot}m^2$) enclosure area. This result exceeds the 5 ach_{50} target for CZ 2. This was followed by multizone/multifan air leakage depressurization guarded testing to quantify zone leakage to exterior versus adjoining zones, as described by Feustel (1989), and Energy Conservatory (2015). The tests revealed significant leakage from the lower attic to the exterior (196 $in.^2$ EqLA [0.13 m^2]). In comparison, the upper attic had 35 $in.^2$ EqLA to the exterior, and the main conditioned space (first and second floors) had 311 $in.^2$ EqLA (0.20 m^2) to the exterior (albeit without door gaskets or finish floors).

Both of these air leakage results indicate that complex details such as roof-to-wall intersections, and conditioned-to-unconditioned attic walls were significant sources of air leakage. However, the field (main body) of the roof and the diffusion vent ridge detail were not significant sources of air leakage. Spray foam unvented roofs are typically very airtight, due to the monolithic air barrier created with the insulation material. In contrast, unvented roofs built with fibrous insulation will likely require greater attention at connection details to achieve equivalent airtightness levels. In hot/humid climates, air leakage may increase attic moisture loads in summer and moderate them in winter.

MONITORING RESULTS: HOUSTON

Overview and Boundary Conditions

Data have been collected in Houston from early February 2014 through June 2016, providing over two years of results and three winters of data.

Exterior climate (based on Houston Intercontinental/IAH airport data) is summarized in Table 5: the first (partial) winter was colder than normal, but the second and third winters were warmer.

Interior conditions were measured at six conditioned attic locations (three high/low pairs) and the interior main space. Attic temperatures ran parallel to interior temperatures, albeit slightly warmer in summer and cooler in winter. Maximum attic-to-interior differences were in the 5°F to 7°F (3°C to 4°C) range. There was a clear diurnal temperature cycle due to solar gain, and there was evidence of vertical temperature stratification. However, a stronger signal was that some portions of the attic were warmer at times of day. This was ascribed to direct solar gain at the west-facing roof plane, and/or the ratio of enclosure gains/losses to incidental conditioning from attic duct leakage.

Conditioned attic dew points were typically between interior and exterior conditions in the summer: a two-week excerpt from July 2014 is shown in Figure 8 (peak summer conditions). The attic runs at a consistently higher dew point than interior, as the space was not directly conditioned or dehumidified. Dew point had a strong diurnal cycle, with peaks occurring between 3 and 6 p.m., which is consistent with moisture adsorbed in sheathing being driven out by solar gain and dry-bulb temperature difference. After sunset, the sheathing tended to adsorb moisture from the air and pull down the dew point as it cooled.

The measurements show moisture stratification in the attic. The highest (south-high) sensor shows the highest peaks; north low and south low sensors showed the lowest peaks.

In the first winter, interior dew points were relatively high, due to completion of construction activities (painting and drywall). In the second winter, dew points were low (40°F–60°F [5°C–15°C]) due to a lack of interior moisture generation. In the third winter, attic dew points were higher, due the addition of humidification at 22.6 lb/day (10.3 L/day), resulting in dew points typically in the 50°F to 63°F/10°C to 17°C range. The attic dew point was higher than interior main space conditions.

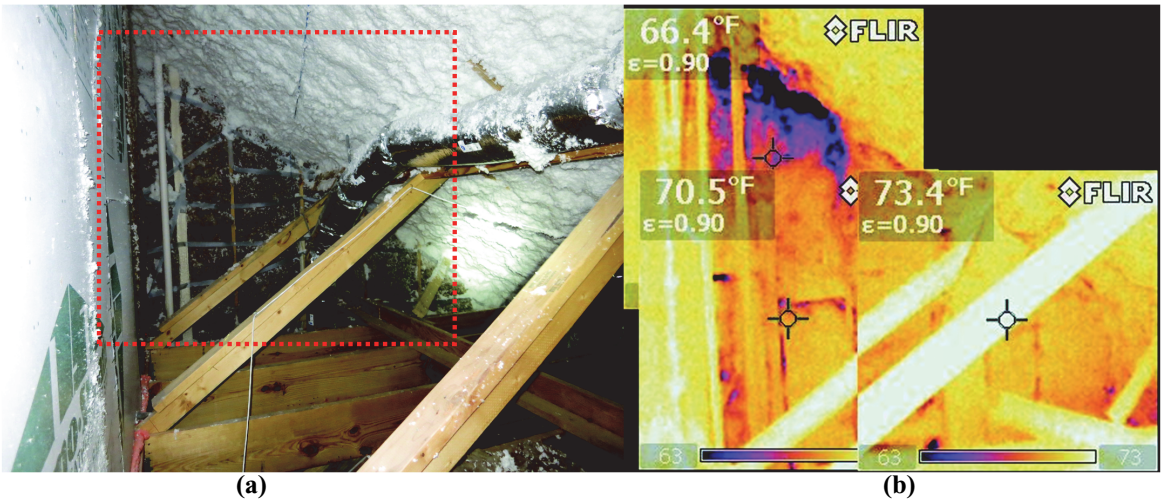

(a) (b)

Figure 7 *Infrared image of Houston attic during air leakage depressurization testing, showing roof-wall air leak.*

Table 4. Orlando (Concrete Tile) Air Leakage Measurements

	cfm_{50} (L/s)	Δ cfm_{50} (L/s)	ach_{50} (h^{-1})	cfm_{50}/ft^2 (L/s·m^2)	EqLA, in^2 (m^2)
Both Hatches Closed	4429 (2090)		6.7	0.51 (2.6)	456 (0.294)
Lower Hatch Open	5012 (2366)	583 (275)	7.6	0.58 (2.9)	516 (0.333)
Upper Hatch Open	4473 (2111)	44 (21)	6.8	0.52 (2.6)	461 (0.297)
Both Hatches Open	5009 (2364)	580 (274)	7.6	0.58 (2.9)	516 (0.333)

Roof Assembly Conditions

Moisture measurements, including RH at the roof peak (moisture accumulation point) and wood MCs throughout the roof could be compared among the experimental assemblies.

Results for a control unvented roof (UVR1) are shown in Figure 9. This and the following plots show roof sheathing and wafer sensor MCs on the left-hand axis. The roof peak RH is plotted on the right hand axis, with a ten-day rolling average superimposed. Roof peak RHs reached high levels (90%+) in the first winter, but as exterior conditions warmed, RHs quickly fell to 40% to 50% due to solar heating driving moisture inward, out of the roof assembly. In the second winter (2014–2015), interior RH levels were low and outdoor conditions mild; RH maxima were much lower (60%–80%), followed by summertime drying. The missing data from April 2015 to August 2015 was due to an instrumentation failure for all RH and MC channels. In the third winter (2015–2016), interior humidification was added, and peak RHs again rose to 90%+ levels. As exterior conditions warmed, RH levels again dropped.

MC measurements were consistent with RH measurements; the first winter MCs were higher than recommended, peaking over 20%, but fell to safe levels (under 10%) in the summer. Similarly, the second winter saw a rise in MCs, but drier than the first winter. The third winter saw a rise in MCs similar to the first winter, with some MC maxima in the 25% to 30% range. The MCs show a spatial pattern, with the highest MCs typically at or near the roof ridge, and higher on the north side than the south side.

A similar plot is shown for an experimental diffusion vent roof (DVR1) in Figure 10. These diffusion vent roofs had a markedly different pattern from the unvented roofs: instead of a seasonal swing, the RH and MC measurements were relatively stable over most of the measurement period. In these roofs, the first winter MCs and RHs were much drier and safer than the unvented roofs. Peak MCs remained lower than 20%. Summertime RHs and MCs are higher than in the unvented roofs, but well within safe conditions. In the second winter (2014–2015), there was a slight rise in RHs

Table 5. Houston (IAH) Exterior Climate HDD/CDD Summary

	HDD, 65°F (18°C)	CDD, 65°F (18°C)	HDD, % of Normal	CDD, % of Normal
Normal (IAH Airport)	1525 (847)	2893 (1607)	—	—
Winter 2013–2014	1739 (966)	—	114%	—
Summer 2014	—	3037 (1687)	—	105%
Winter 2014–2015	1461 (812)	—	96%	—
Summer 2015	—	3344 (1858)	—	116%
Winter 2015–2016	1012 (562)	—	66%	—

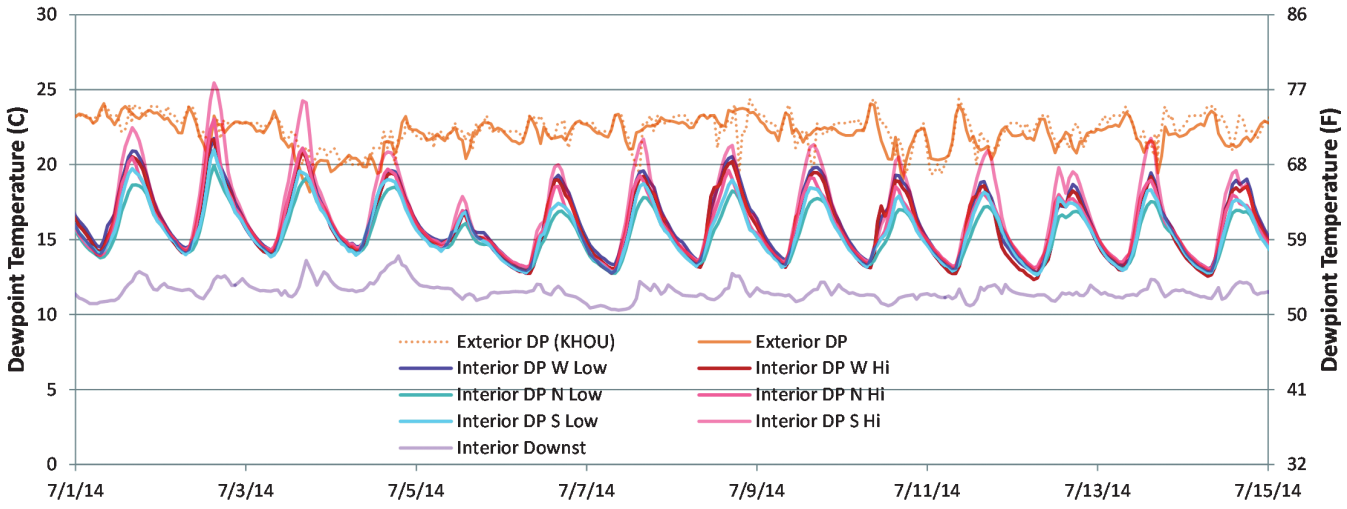

Figure 8 *Houston dew-point temperatures in the summertime (July 2014) detail.*

and wood MCs, but well within the safe range—typically lower than 15%. The third, humidified winter, however, saw a sharp rise in wood MCs. The ridge wafer MC remained low (peaking at 15%), but two north-side sheathing MCs peaked in the 20% to 25% range. This indicates that the diffusion vent provides localized drying at the ridge, but areas away from the diffusion vent may accumulate moisture at high interior RH conditions. As outdoor temperatures warmed, all MC fell back to the safe range.

Roof ridge RH measurements cycled on a diurnal basis; most readings are 50% to 80%. The diurnal RH cycling in the diffusion vent roofs shows a greater range than that in the unvented roofs. When plotted, the roof peak RH shows a consistent sawtooth pattern with a slow rise and a sharp daily fall. The fall in RH coincides with morning solar warming; in the late afternoons (sunset) the RH started to rise, continuing overnight into the morning. The MCs had a similar type of sawtooth behavior but over a much smaller range.

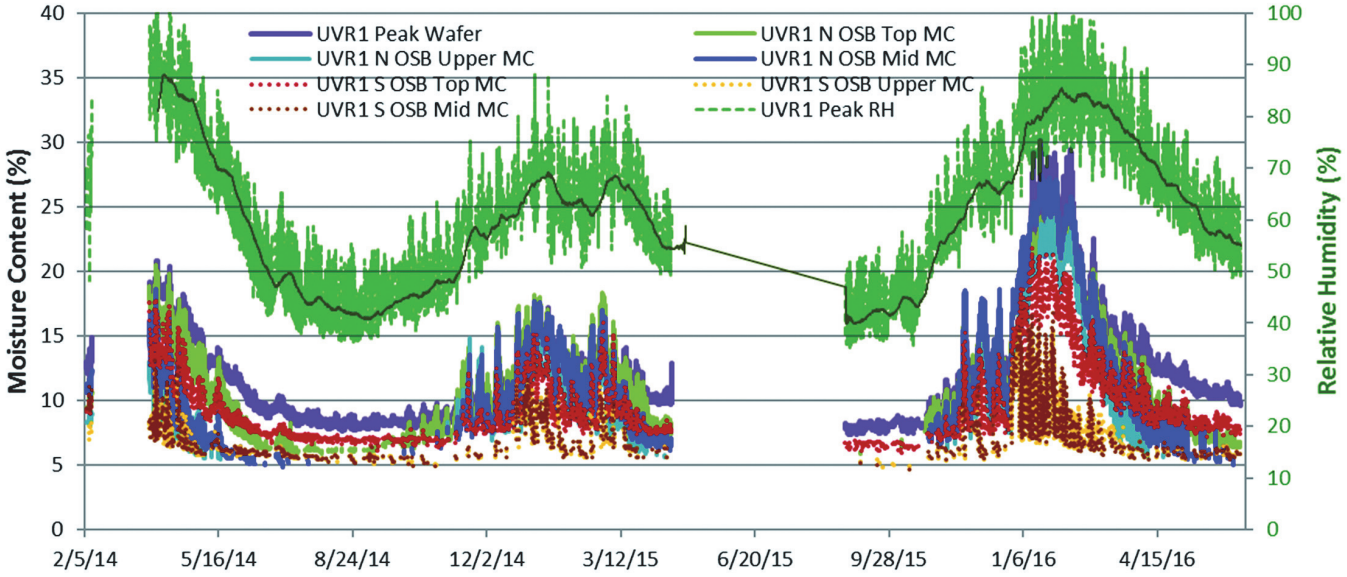

Figure 9 *Houston unvented roof (UVR1) roof MC and RH measurements.*

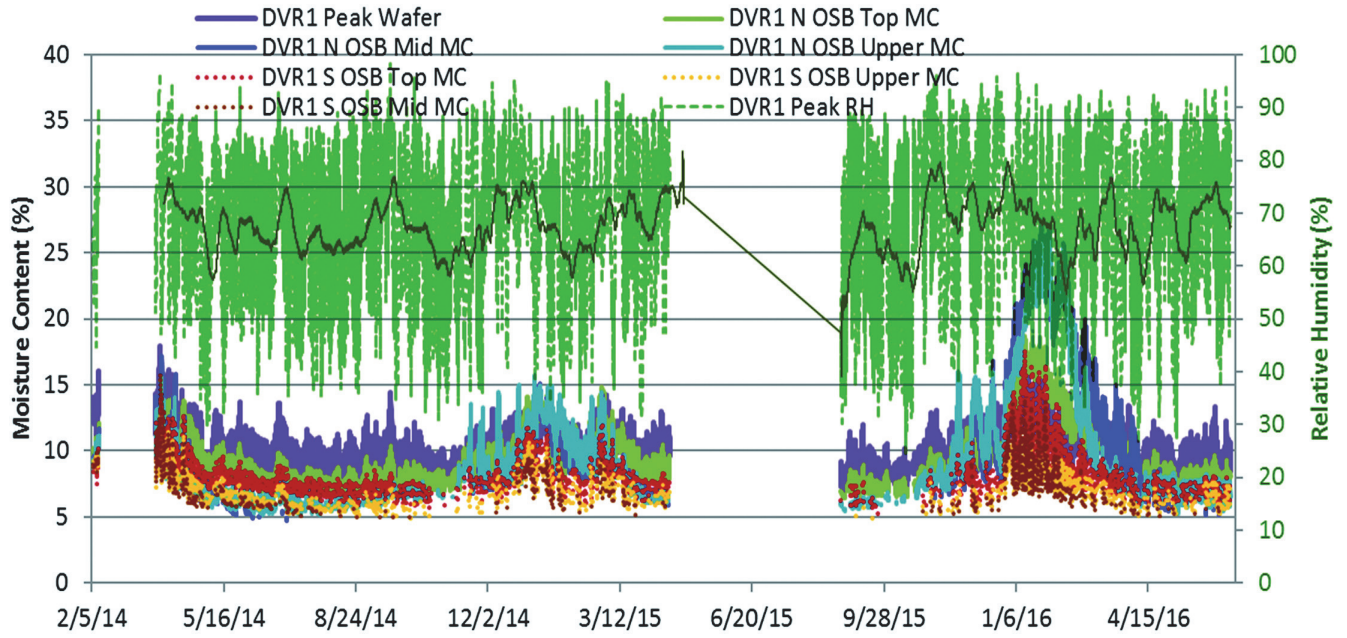

Figure 10 *Houston diffusion vent roof (DVR1) roof MC and RH measurements.*

Two monitored locations were hip geometries (DVH4 and DVH5); the hips are different from the ridge diffusion vents because the diffusion vent area is smaller (2 in. [51 mm] diameter drilled holes near the peak). These roofs exhibit behavior partway between the unvented and diffusion vent roofs, consistent with the reduction of exposed diffusion drying area.

The two roof systems (UVR1 and DVR1) are plotted together in Figure 11, isolating ridge RH and the wafer sensor at the ridge. A comparison of RH patterns shows that the unvented roof has higher RHs in winter during high dew-point conditions and lower in summer, while the diffusion vent roof has high variability but lower wintertime peaks. A similar pattern is seen at the ridge wafers: unvented roof is wetter in winter and drier in summer. The wafer sensor is useful in that it maps to long-term moisture accumulation patterns and, hence, the potential for moisture damage.

These patterns are shown Figure 12, which shows five-day details of summer behavior (August 2014, Figure 12a) and winter behavior under humidified conditions (February 2016, Figure 12b).

During the summer, unvented RHs are lower (35%–55%) than diffusion vent RHs (40%–90%). The greater diurnal cycling of the diffusion vent roof is evident, due to the coupling to exterior conditions at the vapor-open membrane. It results in greater drying during daytime heating and moisture uptake at night. However, the ridge wafers show that overall accumulation at the ridge is negligible in both roofs, with MCs in the 8% to 11% range.

In contrast, in winter, the unvented roof shows greater long-term moisture accumulation at the ridge wafer (20%–30% MC), while the diffusion vent ridge remains in the safe 10% to 14% range. Unvented roof RHs show peak levels hitting 100% rh at midday conditions, likely due to trapped moisture being desorbed from the sheathing.

The field monitoring work covered eight roof locations. To summarize the data, results are presented as box-and-whisker plots that show the overall range and distribution of measurements. The box-and-whisker plots show median (center of box), lower and upper quartile of data (extent of box), and maximum/minimum (extension lines). The ridge RHs are shown in Figure 13a and wafer MCs in Figure 13b. Given the varying boundary conditions, the final season (August 2015–June 2016) is plotted, which reflects humidified winter conditions.

There is substantial overlap between the unvented and diffusion vent roofs. The median and quartile RHs are higher in the diffusion vent roofs; this is consistent with the lack of seasonal wet-dry swings (i.e., DVR RHs remain higher in summer). However, DVR1, 2, 3, and 6 have lower maxima than UVR1 and 2.

The wafer MCs provide an indication of long-term moisture accumulation, indicating higher outliers in the unvented roof assemblies; the diffusion vent roofs have consistently lower maxima, except for DVH5. During decommissioning, DVH5 was found to have been assembled incorrectly, with the diffusion vent ports constricted by vapor-impermeable layers.

ASHRAE Standard 160 (ASHRAE 2009, 2011) provides guidance on moisture analysis for building envelope design, including the moisture performance evaluation criteria. Moisture failure criteria are defined as hours with a "30-day running average surface RH over 80% when the 30-day running average surface temperature is between 5°C and 40°C (41°F and 104°F)" (ASHRAE 2011). Failure criteria for the assemblies were calculated using 30-day running averages of the ridge RH and temperature; hourly pass/fail results (i.e., hours with likely mold growth) were tabulated. This analysis showed that both unvented roof assemblies (UVR1/UVR2) had hours failing ASHRAE Standard

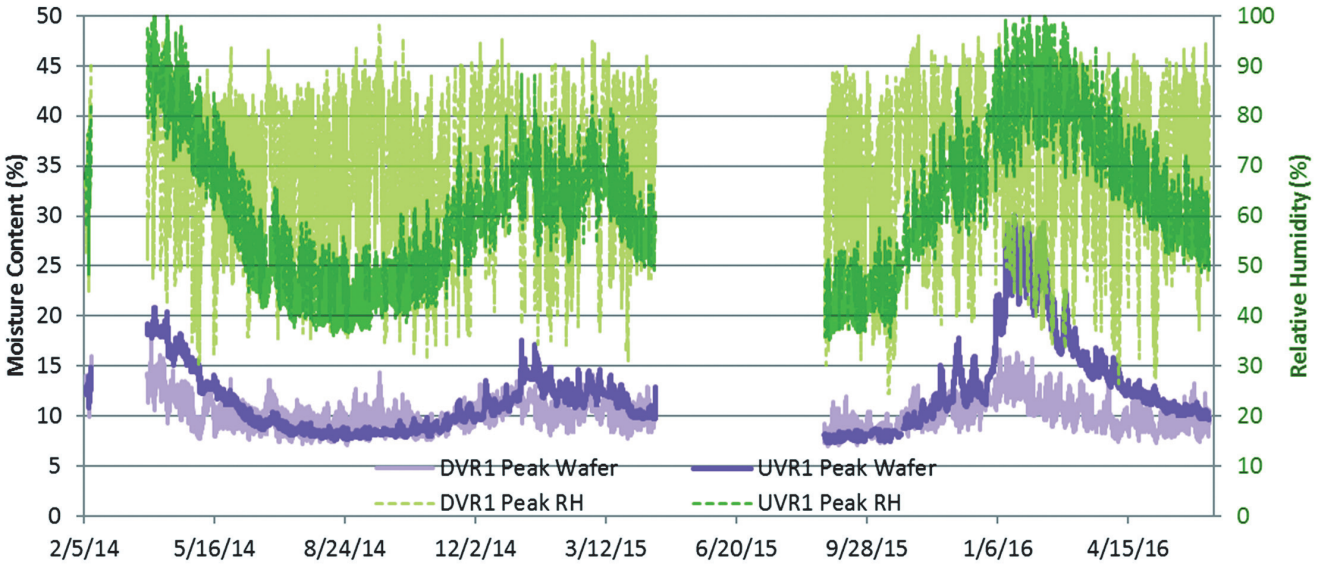

Figure 11 *Houston unvented (UVR1) and diffusion vent (DVR1) roof wafer MC and RH comparison.*

160 criteria in the first partial winter (427 and 238 hours, respectively); no diffusion vent roofs had failing hours. Admittedly, ASHRAE Standard 160 is known to provide overly stringent failure criteria (i.e., provides false positives of failure).

Overall, these results indicate that the diffusion vent roof had less wintertime moisture accumulation than the unvented roof and the potential for avoiding the ridge rot failures seen in the field in earlier work.

Inward Drive Experiment

Capillary water accumulation in shingle laps and inward solar moisture vapor drives have been suggested as contributors to unvented attic humidity problems. However, this mechanism was refuted by hygrothermal modeling by Boudreaux et al. (2013) and by a field comparison of roof underlayments by Lstiburek (2014). However, given this opportunity, the issue was studied further in Houston: a 2 ft (610 mm) square section of south-facing roof was isolated using 1 in. (25 mm) foam blocking covered with construction tape to reduce its vapor permeance (Figure 14a). After insulation, the interior side was covered with a layer of 0.093 in. (2.4 mm) clear acrylic plastic and air sealed at the perimeter with flashing tape (Figure 14 b).

Instrumentation included sheathing MC/T and interior-side RH/T and wafer sensors (Figure 14 right). The intent was to capture moisture that was driven through the exterior side of the assembly (shingles, underlayment, and sheathing) into the insulated, sealed cavity. Inward-driven moisture would accumulate at the insulation-to-acrylic plastic interface and was measured by the T/RH and wafer sensors. Sheathing MC was measured to determine whether moisture within the closed system increased over time as moisture was driven from one side to the other seasonally. This experiment was not intended to capture any diurnal or seasonal increase of MCs due to accumulated interior-sourced moisture in the sheathing. Instead, it

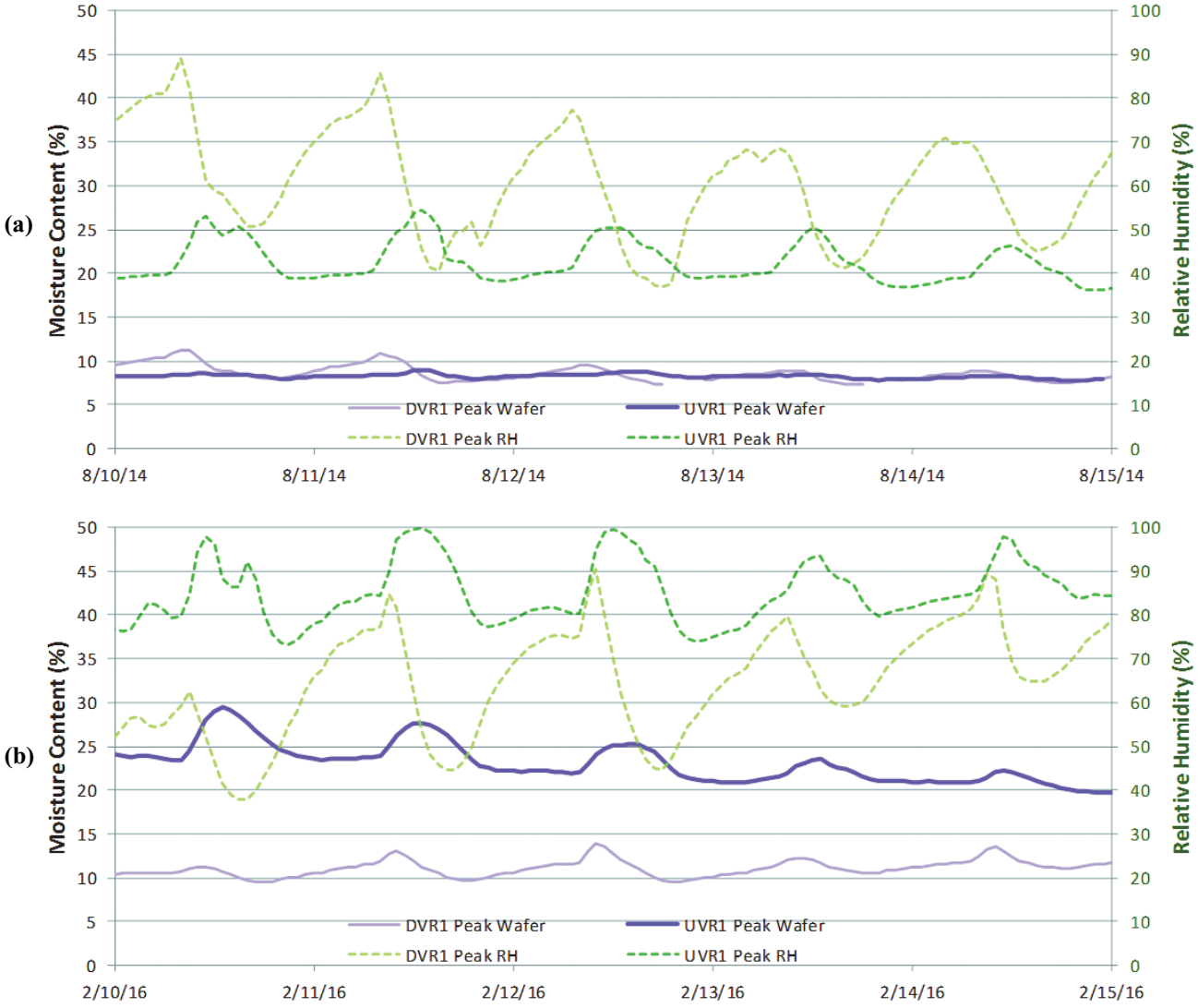

Figure 12 *Houston unvented and diffusion vent wafer MC and RH in (a) summer and (b) winter, five-day details.*

was intended to only capture inward-driven moisture from the exterior source. The initial sheathing MC was measured with a handheld meter at 8% to 9% MC.

Selected data are shown in Figure 15; the interior-side RH cycles seasonally (higher in summer) and daily, due to solar gain. Summertime peaks over 90% occur, but with no evidence of condensation (100% rh). Comparable data were measured by the interior wafer sensor. The wafer results were examined for correlations with exterior weather events: interior and exterior dew point had weak relationships. Precipitation was also plotted for correlation, given that wetted shingles are a suspected moisture source for inward drive. Although some wafer MC spikes correlated with precipitation, many other events were uncorrelated. The tightest correlation of boundary conditions to wafer response was the 24-hour average of the exterior sheathing temperature; there is excellent correlation to the MC rise and fall patterns. This is consistent with solar-heated sheathing desorbing moisture that is driven to the interior side. The wafer MCs rise and fall within a fixed range, indicating that moisture is not being added to the closed" system. The exterior sheathing MC was compared with other sensors in the same roof; similar MC levels were seen, also indicating a lack of moisture gain.

Overall, the lack of high moisture levels (condensation/100% rh) and the stable interior and exterior MC ranges (i.e., no ratcheting increase of moisture) point away from inward moisture vapor drives as a mechanism that adds humidity to the attic. This is consistent with Künzel and Sedlbauer's (2001) measurements of compact (cathedral cellulose) roof assemblies with clay and concrete barrel tile near Munich, Germany (roughly CZ5). A strong inward vapor drive effect was seen in summertime in the south-facing clay tile roof (30%+ MC at the rafters), but no effect was seen in the concrete tile roof. This effect was ascribed to the difference in water uptake or water absorption coefficient; concrete tile is much less absorptive than clay tile. The minimal storage and absorption in asphalt shingle roofing is consistent with the field results.

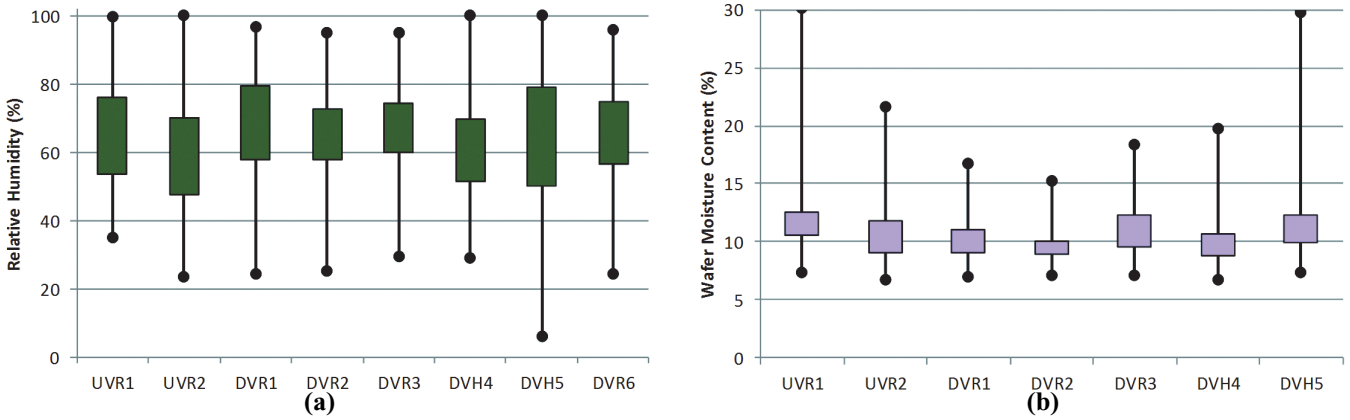

Figure 13 *Houston box-and-whisker plots for roof ridge moisture conditions: (a) RH and (b) wafer MC August 2015 to June 2016.*

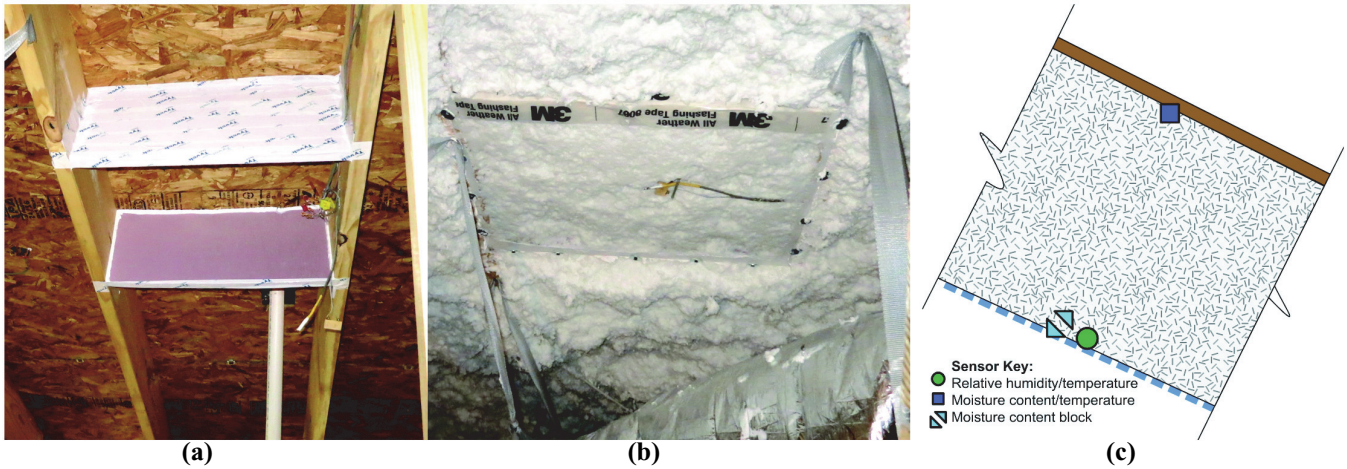

Figure 14 *Inward drive box (a) before and (b) after insulation and clear plastic cover and (c) sensor package.*

MONITORING RESULTS: ORLANDO

Overview and Boundary Conditions

Data have been collected in Orlando from early November 2014 through June 2016, providing roughly 20 months of results and two winters of data, with one partial winter. Exterior climate taken from Orlando airport data is summarized in Table 6. Both winters had lower than normal heating degree days and summers with higher than normal CDD. Although both locations are in CZ 2A, the heating load in Orlando is much smaller than Houston (580 versus 1525 HDD 65°F [322 versus 847 HDD 18.3°C], respectively). The difference is also demonstrated by wintertime 99.6% design heating temperatures (37.7°F [3.2°C] Orlando versus 29.1°F [–1.6°C] Houston), per climate data in ASHRAE (2013). Of course, with milder/warmer winters, interstitial condensation problems are reduced. Humidity loads between the two locations are more comparable; 0.4% design dew-point temperatures are 77.6°F [25.3°C] Orlando and 77.9°F [25.5°C] Houston (ASHRAE 2013).

Interior temperature and RH in the conditioned attics were measured at six points; one high/low pair in the attic above the second floor and two high/low pairs in the attic above the first floor. Patterns were similar to the Houston monitoring: attic temperatures ran parallel to interior (main space) conditions. However, attic temperatures were warmer in summer, and cooler in winter, with maximum excursions in summer of 7°F [4°C]. In summer, the second floor attic tracked warmer than others; in winter the second floor attic and the exposed front first floor attic tracked colder than interior. Paired sensors indicated temperature stratification in the attics.

Dew points in the attic (Figure 16) were substantially higher than the interior main space in the summer, with peak dew-point differences/excursions in the 27°F (15.2°C range). Attic dew points showed a strong diurnal swing, consistent with moisture being adsorbed and desorbed from the roof sheathing. The second floor attic consistently had the highest summertime dew points; air leakage testing indicated that this attic was much tighter than the first floor attic. This result is consistent with moisture stratification within the house driv-

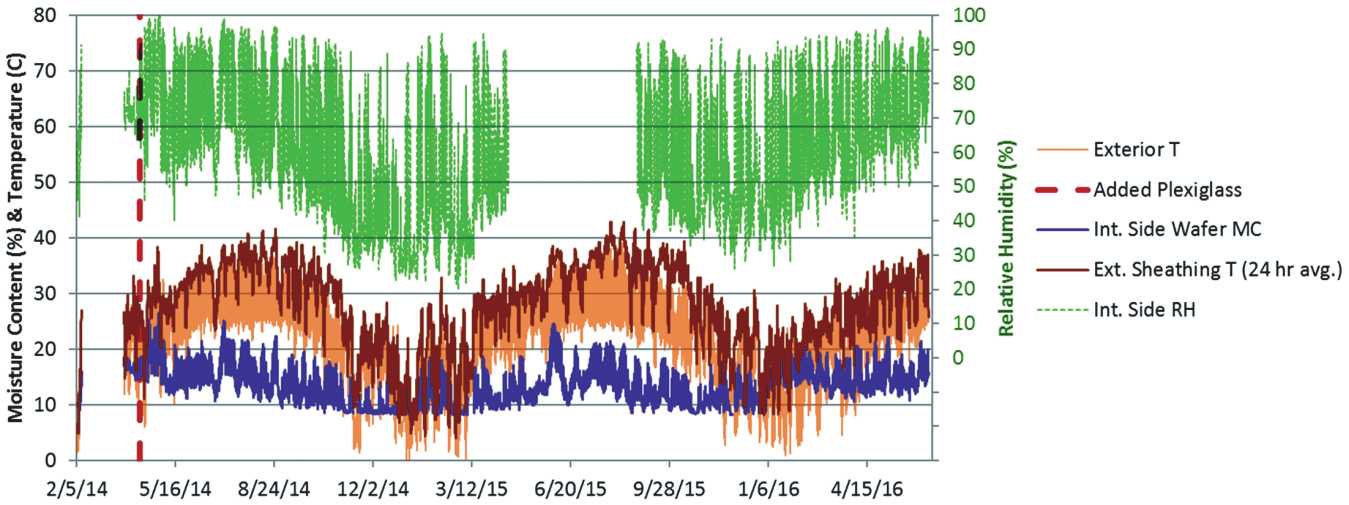

Figure 15 *Inward drive data, including interior-side RH and wafer MC, exterior T, and exterior sheathing T (24-hour rolling average).*

Table 6. Orlando (MCO) Climate HDD/CDD Summary

	HDD, 65°F (18.3°C)	CDD, 65°F (18.3°C)	HDD, % of Normal	CDD, % of Normal
Normal	580 (322)	3428 (1904)	—	—
Winter 2013–2014	410 (228)	—	71%	—
Summer 2014	—	3573 (1985)	—	104%
Winter 2014–2015	497 (276)	—	86%	—
Summer 2015	—	4266 (2370)	—	124%
Winter 2015–2016	378 (210)	—	65%	—

ing attic humidity levels, rather than exterior air leakage as the primary factor. Attic dew-point measurements again showed strong signs of vertical stratification.

Roof Assembly Conditions

RH measurements at the roof peak and wood MCs throughout the roof were plotted in a similar manner to the Houston roof; Orlando results for the unvented roof and diffusion vent roof are shown in Figure 17 and Figure 18, respectively. The gap in data (winter 2014–2015) was due to site power issues; moisture-generating construction activities (gypsum board finishing and painting) occurred during this period.

In the unvented roof, similar to Houston work, ridge RHs in the first winter were high (90%–100%); the ridge wood wafer sensor peaked over 30% (indicating possible condensation). However, RH and MCs dropped rapidly in summer to safe levels, due to the inward temperature gradient. In the second winter, RHs and MCs rose to similar levels, with RH peaks near 100% for extended periods.

Similar to Houston, the diffusion vent roof shows less of a seasonal RH swing (with only brief excursions over 90% RH) and lower peak wood MCs. Wood MCs hit a maximum of 18% at the ridge sheathing, and 15% in other roof locations.

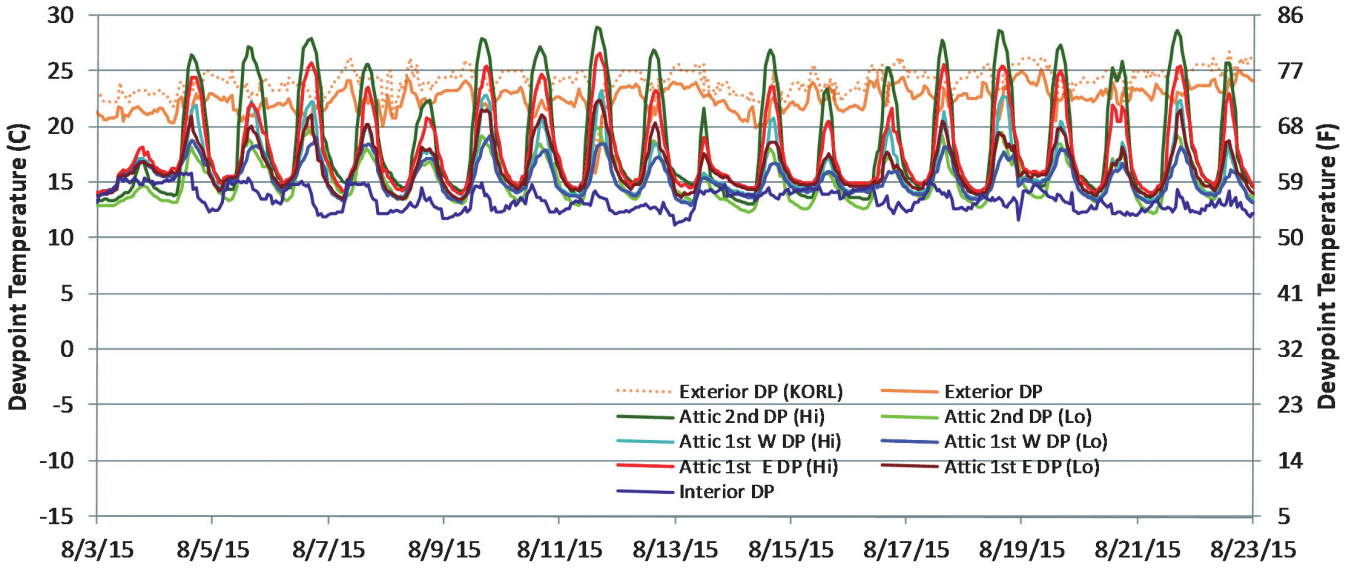

Figure 16 *Orlando unvented attic summertime (August 2015) dew points, with interior and exterior dew point.*

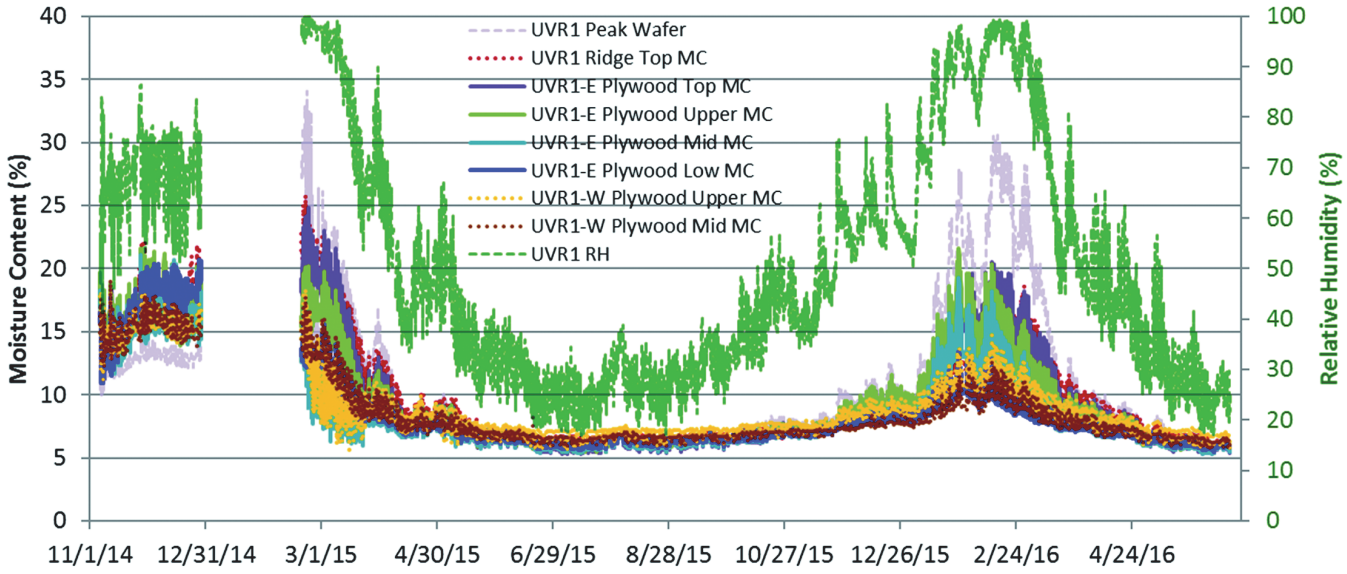

Figure 17 *Orlando unvented roof (UVR1) roof MC and RH measurements.*

Again, the two roofs were plotted together (RH and wafer MC) in Figure 19, allowing direct comparison; the higher RHs and MCs in the unvented roof ridge during the first winter are evident.

The eight experimental roofs are compared with box-and-whisker plots, showing ridge RH (Figure 20a) and wafer MC (Figure 20b) for the entire monitoring period.

There was only one unvented control roof at this test site; there were diffusion vent ridges and hips (DVR/DVH) and two roof-wall (RW) intersections (no diffusion vent). Similar to the Houston roof, the diffusion vent roofs showed a higher median and distribution of RHs than the unvented roof, but the unvented roof had the highest wintertime excursions. The wafer MC data shows the strong effect of the winter outliers in the unvented roof.

One hip measurement (DVH2) and two roof-wall measurements (RW1/RW2) have higher RH and wafer MC distributions than the remaining diffusion vent roofs. This is likely due to the shading patterns created by the building, as shown in Figure 21. The lower diffusion vent hip measurement (DVH1) is fully exposed to the sun, while the upper measurement (DVH2) is shaded by the adjacent second story and roof. The roof-wall interfaces (RW1 and RW2) lie directly north of the wall in shadow.

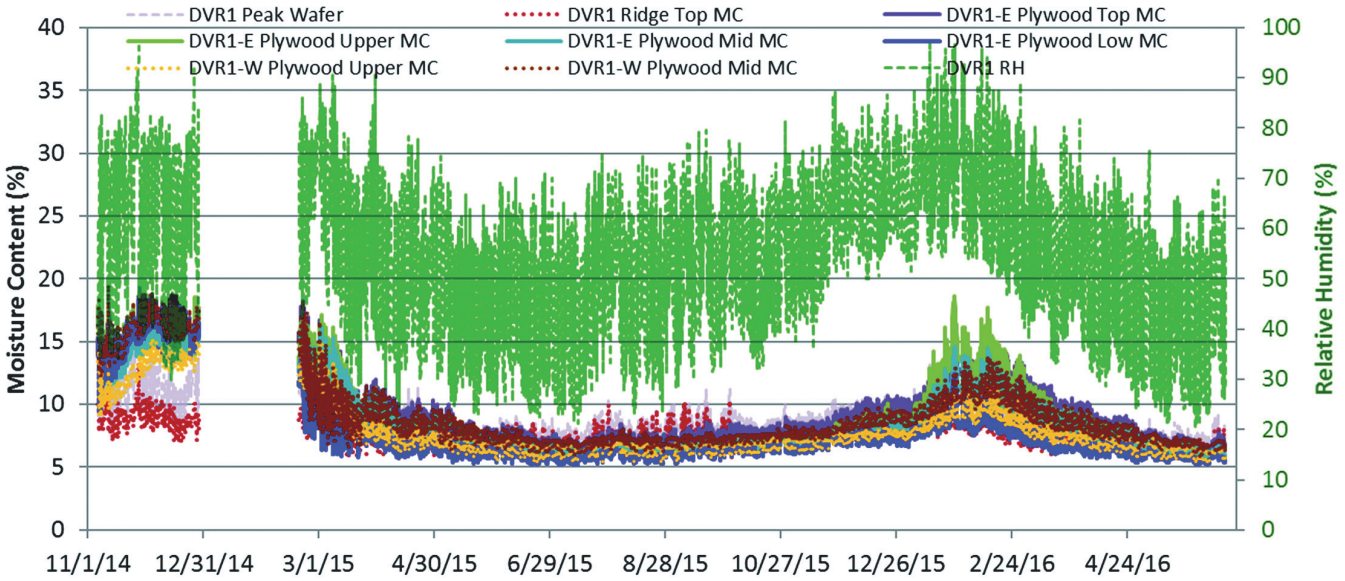

Figure 18 *Orlando diffusion vent roof (DVR1) roof MC and RH measurements.*

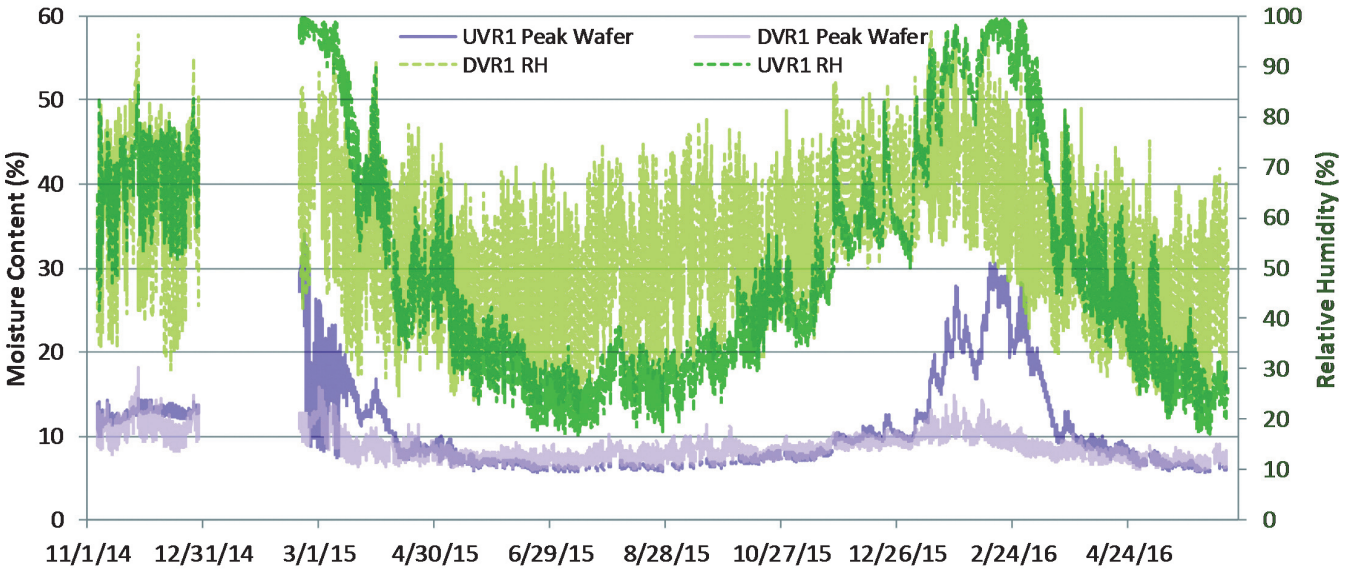

Figure 19 *Orlando unvented (UVR1) and diffusion vent (DVR1) roof wafer MC and RH comparison.*

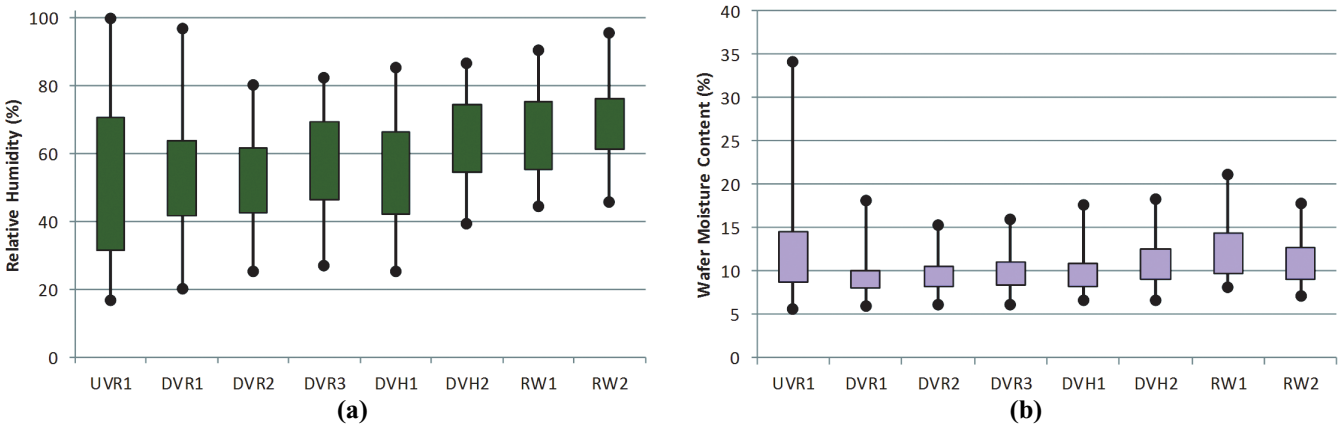

Figure 20 *Orlando box-and-whisker plots for roof ridge moisture conditions: (a) RH and (b) wafer MC.*

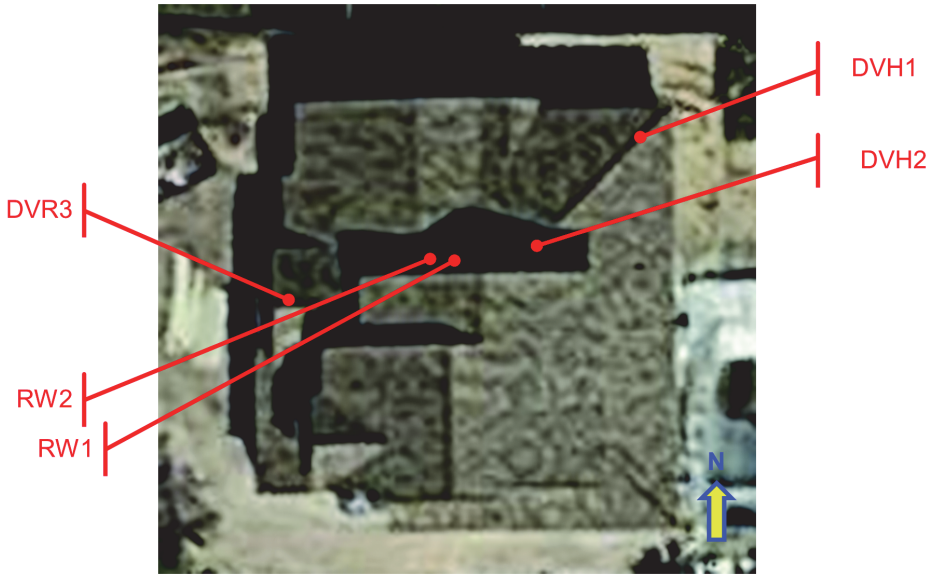

Figure 21 *Overhead view of roof shading with key sensor locations.*

This was confirmed by plotting roof sheathing temperatures at these locations; this shading resulted in cooler sheathing temperatures. In addition, these temperatures did not show the same diurnal cycling as in the exposed roofs.

Most of the roofs have hours with ridge RH measurements that exceed 80% rh. However, given the discontinuity (missing portion) of data, an ASHRAE Standard 160 analysis (ASHRAE 2009, 2011), which relies on 30-day rolling averages, does not provide useful information.

DECOMISSIONING AND DISASSEMBLY

At the conclusion of the experiment, the data logging equipment was removed, and the experimental unvented (self-adhered membrane) portions were retrofitted with the diffusion vent detail. Interior and interstitial conditions were examined during this final visit.

In the Houston (asphalt shingle) house, no visible signs of moisture damage were seen from the interior or during partial exterior roof disassembly. However, insulation was not removed from roof bays, limiting surveys of the framing and sheathing conditions. DVH5 was found to have shingles overlapping the diffusion vent port (Figure 22), explaining measurements similar to the unvented roof assemblies. Shingles were cut away to open the diffusion vents to the exterior.

In the Orlando (tile roof) house, spotting (likely mold) was seen on the interior insulation netting at the peak/ridge, tapering in intensity coming down the roof, extending roughly 4 ft (1.2 m) downslope (Figure 23). This issue was only seen at the highest ridge (upper attic, or UVR1/DVR1). Spotting was also seen at the top end of the wood truss vertical member, typically where covered by insulation netting (Figure 23a). The truss spotting was only seen at the

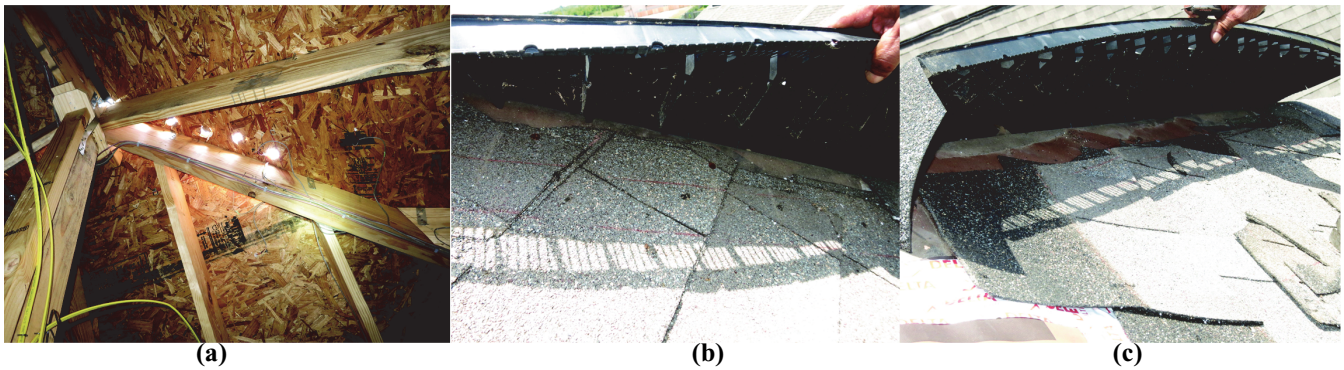

Figure 22 *Houston (a) roof hip diffusion vent holes, (b) DVH-5 blocked by shingles, and (c) retrofit.*

Figure 23 *Orlando tile roof interior conditions showing spotting on insulation netting and truss vertical member.*

unvented roofs, and not at the diffusion vent roofs. This growth is entirely consistent with measured moisture accumulation in the upper attic during the first winter, due to construction moisture. This moisture then became vertically stratified in the attic, resulting in condensation on upper netting and truss surfaces. Truss spotting occurred only in the unvented attic, due to greater local accumulation than the diffusion vent roof. Infrared observations showed that truss spotting is consistent with thermal bridging. The monitored data show the problems occurred in the first winter but did not recur in the second winter. These observations are entirely consistent with previous field observations of unvented attics with fibrous insulation.

Temperature and moisture (dew point) stratification were also directly measured in attics at both sites with a handheld meter. Measurements showed stratification consistent with the long-term monitoring patterns.

ANALYSIS AND CONCLUSIONS

Two unvented or conditioned attic houses were monitored in CZ 2A; key points from the data include the following.

Both unvented attics ran at temperature conditions near interior setpoint; daily temperature excursions ran high in summer and cool in winter. Attic conditions result from the balance of enclosure losses/gains (conductive, solar gain, and air leakage) versus conditioning losses/gains from duct leakage, air leakage from interior space, and conduction.

Attic dew points also showed strong daily cycling that was consistent with desorption (during the day) and adsorption (at night) of moisture from the roof sheathing. Sheathing adsorption/desorption is likely greater in roofs than walls due to color (often dark) and orientation (assembly experiences direct solar gain and night-sky cooling). These effects are intensified with the use of vapor- open insulation materials (open-cell polyurethane spray foam or fibrous insulation) and when an interior air barrier and vapor retarder are not used (per these test roofs).

Interior dew-point peaks were at times higher than outdoor dew-point conditions; Lstiburek (2014) recommends intentional space conditioning of the attic space to provide dehumidification. Both temperature and dew point showed vertical stratification, which is consistent with the concentrated moisture issues seen at the roof ridge/highest point.

The unvented roof assemblies had a strip of vapor-impermeable (Class I vapor barrier), self-adhered membrane at the ridge; the resulting assembly is moisture-coupled only to interior conditions. During the summer, the thermal gradient drives stored moisture inward, out of the assembly, resulting in dry conditions. In winter, when interior dew points are suffi-

ciently elevated, moisture accumulation occurs at the ridge; wintertime peaks were much higher than 20% MC. For reference, decay fungi are inhibited when MC is lower than 20% (FPL 2010); optimum growth occurs in the 25% to 30% MC range. However, at drier interior conditions, moisture accumulation was minimal and well within the safe range. In the following spring, with warmer weather, the roof dried to safe levels. Moisture accumulation issues were seen primarily at the high points of the roof assembly (e.g., ridge); these issues were not seen in lower portions. Wood MCs were consistent with RH measurements.

In contrast, the diffusion vent roofs had a strip of vapor-permeable membrane at the opening; ridge conditions are coupled to both interior and exterior conditions, creating a flow-through assembly. Moisture can adsorb from and desorb to both the interior and exterior. The resulting ridge RH conditions showed strong diurnal oscillations. Higher RHs were seen in the diffusion vent roof in summertime (than the unvented roof) but within the safe range. Drier conditions were seen in the diffusion vent roof in wintertime, due to the outward drying of the moisture accumulating at the ridge.

The results collected to date show moisture accumulation at the unvented roof ridges, but the levels did not create catastrophic failures, based on decommissioning observations. However, the accumulation is consistent with the failures seen in previous field work on unvented attics with fibrous insulation. High interstitial moisture levels were seen in the first winter of operation, which involved drying of construction moisture; this is consistent with the timing of the failures seen historically in the field. With interior humidification, the Houston diffusion vent roof showed greater drying and less moisture accumulation than the unvented roof. Even if actual failures did not occur in the test roofs, results indicate that the diffusion vent assembly has a greater margin of safety than an unvented assembly with vapor-impermeable materials at the ridge.

A study of the solar inward-driven moisture through asphalt roof shingles in Houston indicated that no moisture accumulation was occurring due to inward drives. Instead, the fixed amount of moisture within the closed test assembly was driven to the interior or exterior due to the thermal gradient; the moisture levels seen at the interior side closely tracked exterior roof sheathing temperature.

FURTHER WORK

Overall, the use of a diffusion vent at the roof ridge appears to be a promising technology, especially in milder climate zones. The test climates (Houston and Orlando; CZ 2A) are not highly challenging for wintertime condensation but were selected because problems were previously observed in the field using these assemblies in these climates.

Of course, in colder climate zones, interstitial condensation risks increase. These risks might be counteracted by interior airflow and vapor flow control; in these test roofs, no attempt was made to control air or moisture vapor at the interior side of the assembly. In addition, as seen in the collected data, interior dew point affects the level of moisture risk. Unvented roof assemblies using fibrous insulation and interior air/vapor control will be studied in future research.

ACKNOWLEDGMENTS

The authors would like to thank the U.S. Department of Energy's Building America Program for funding the research underlying this paper. This research was also made possible by generous donations of materials, access to test buildings, and support by Cosella Dörken, David Weekley Homes, DuPont Building Innovations, Johns Manville, and Owens Corning.

REFERENCES

ASHRAE. 2009. ANSI/ASHRAE Standard 160-2009, *Criteria for moisture-control design analysis in buildings*. Atlanta: ASHRAE.

ASHRAE. 2011. ANSI/ASHRAE Standard 160-2009, *Criteria for moisture-control design analysis in buildings*, Addendum a. Atlanta: ASHRAE.

ASHRAE. 2013. *ASHRAE Handbook—Fundamentals*. Atlanta: ASHRAE.

Boudreaux, P., S. Pallin, and R. Jackson. 2013. *Moisture Performance of Sealed Attics in the Mixed-Humid Climate*. Technical Report ORNL/TM-2013/525. Oak Ridge, TN: Oak Ridge National Laboratory, Energy and Transportation Science Division.

Energy Conservatory. 2012. Minneapolis Blower Door™ Operation Manual for Model 3 and Model 4 Systems. http://www.energyconservatory.com/sites/default/files/documents/mod_3-4_dg700_-_new_flow_rings_-_cr_-_tpt_-_no_fr_switch_manual_ce_0.pdf.

Energy Conservatory. 2015. General Guarded Blower Door Testing Guidance. http://energyconservatory.com/wp-content/uploads/2015/01/General-Guarded-Blower-Door-Testing-Guidance.pdf.

Feustel, H.E. 1989. Measurements of air permeability in multizone buildings. *Energy and Buildings* 14:103–16.

FPL. 2010. *Wood Handbook—Wood As an Engineering Material*. Technical Report, FPL-GTR-190. Madison, WI: U.S. Department of Agriculture, Forest Service, Forest Products Laboratory.

ICC. 2009. *2009 International Residential Code for One- and Two-family Dwellings*. Country Club Hills, IL: International Code Council.

ICC. 2012. *2012 International Energy Conservation Code*. Country Club Hills, IL: International Code Council.

Künzel, H., and K. Sedlbauer. 2001. Steildächer-feuchte- und wärmetechnische Ausbildung. Bauphysik-Kalendar, Ernst & Sohn, 13086 Berlin, S. 459–82.

Lstiburek, J. 2006. Understanding attic ventilation. *ASHRAE Journal* 48(4):36–38, 40, 42–45. Atlanta: ASHRAE. https://buildingscience.com/documents/digests/bsd-102-understanding-attic-ventilation.

Lstiburek, J. 2010. Building sciences: Don't be dense with insulation. *ASHRAE Journal* August, 54–57. Atlanta: ASHRAE. https://buildingscience.com /documents/insights/bsi-043-dont-be-dense.

Lstiburek, J. 2011. A crash course in roof venting. *Fine Homebuilding Magazine* August/September, 68–72. Newtown, CT: Taunton Press. www.buildingscience. com/documents/published-articles/pa-crash-course-in -roof-venting/view.

Lstiburek, J. 2014. Building sciences: Cool Hand Luke meets attics. *ASHRAE Journal* April, 52–57, Atlanta: ASHRAE. www.buildingscience.com/documents /insights/bsi-077-cool-hand-luke-meets-attics.

Owens Corning Insulating Systems, LLC. 2015. Owens Corning PROPINK® High Performance Conditioned Attic System Installation Guidelines, Pub No. 10019449-B. October 2015. http://www2.owenscorning.com/literature /pdfs/HPCA%20Installation%20Instructions.pdf. Accessed January 2016.

Pallin, S., P. Boudreaux, and R. Jackson. 2014. Indoor climate and moisture durability performances of houses with unvented attic roof constructions in a mixed-humid climate. Technical Report ORNL/TM-2014/549. Oak Ridge, TN: Oak Ridge National Laboratory, Energy and Transportation Science Division.

Rose, W., and D. McCaa. 1998. Temperature and moisture performance of wall assemblies with fiberglass and cellulose insulation. *Proceedings: Thermal Performance of the Exterior Envelopes of Buildings VII*, 133–44. Atlanta: ASHRAE. ISBN 1-883413-70-2.

Rudd, A.F., and J.W. Lstiburek. 1998. Vented and sealed attics in hot climates. *ASHRAE Transactions*. TO-98-20-3.

Salonvaara, M., A. Karagiozis, and A. Desjarlais. 2013. Moisture performance of sealed attics in Climate Zones 1 to 4. *Proceedings: Thermal Performance of the Exterior Envelopes of Buildings XII*. Atlanta: ASHRAE.

Schumacher, C.J., and R. LePage, R. 2012. BA-1308: Moisture control for dense-packed roof assemblies in cold climates: Final measure guideline. www.buildingscience.com /documents/bareports/ba-1308-moisture-control-dense -packed-roof-assemblies-cold-climates/view.

Straube, J., D. Onysko, and C. Schumacher. 2002. Methodology and design of field experiments for monitoring the hygrothermal performance of wood frame enclosures. *Journal of Thermal Envelope and Building Science* 26(2).

Ueno, K., and J. Straube. 2008. Laboratory calibration and field results of wood resistance humidity sensors. *Proceedings of BEST 1 Conference*, Minneapolis, June 10–12.

Ueno, K., and J.W. Lstiburek. 2015a. Field testing unvented roofs with asphalt shingles in cold and hot-humid climates. U.S. Department of Energy/Building America Report DOE/GO-102015-4705. http://www.nrel.gov /docs/ fy15osti/64543.pdf.

Ueno, K., and J.W. Lstiburek. 2015b. Field testing of an unvented roof with fibrous insulation, tiles, and vapor diffusion venting. U.S. Department of Energy/Building America Report DOE/GO-102015-4764. http:// apps1.eere.energy.gov/buildings/publications/pdfs /building_america/64999.pdf.